

Shear viscosity of QGP and the anisotropic flows within an event by event transport approach

S. PLUMARI^{1,2}, G. L. GUARDO², A. PUGLISI^{1,2}, F. SCARDINA^{1,2} and V. GRECO^{1,2}

¹Department of Physics and Astronomy, University of Catania,
Via S. Sofia 64, I-95123 Catania, Italy

²INFN-Laboratori Nazionali del Sud, Via S. Sofia 62, I-95123 Catania,
Italy

Abstract

We have employed a relativistic kinetic transport approach that incorporates initial state fluctuations to study the effect of a temperature dependent shear viscosity to entropy density ratio $\eta/s(T)$ on the build-up of the anisotropic flows $v_n(p_T)$. We find that at LHC energies and for ultra-central collisions ($0 - 0.2\%$) the $v_n(p_T)$ have a stronger sensitivity to the T dependence of η/s in the QGP phase and this sensitivity increases with the order of the harmonic n . Moreover we have studied the correlation between the initial spatial anisotropies ϵ_n and the final flow coefficients $\langle v_n \rangle$ for different centralities and for the two beam energies. The study shows that at LHC energies there is more correlation than at RHIC energies. In particular at LHC energies and for ultra-central collisions the linear correlation coefficient $C(\epsilon_n, v_n) \approx 1$ for $n = 2, 3, 4$ and 5 suggesting that the $\langle v_n \rangle$ are strongly related to the initial value of ϵ_n .

1 Introduction

One of the most surprising results obtained in the experiments conducted at RHIC and more recently at the LHC is that the matter created in these

heavy ion collisions behaves as an almost perfect fluid with a very low η/s ratio. The observable indicating such a low value for η/s is the so called elliptic flow, v_2 . The elliptic flow is the second coefficient in the Fourier expansion of the azimuthal angle distribution of emitted particles and it a measure of the azimuthal asymmetry in momentum space. The determination of the η/s ratio of the QGP is one of the main challenges in the relativistic heavy ion physics. The comparison between experimental data and theoretical calculations within viscous hydrodynamics and transport approach [1–4] have shown that this large value of v_2 is consistent with a very low η/s . The average value extracted is close to $1/(4\pi)$ which is the lower bound conjectured for strongly interacting systems, $\eta/s = 1/4\pi$ [5].

The possibility to measure event-by-event the angular distribution of emitted particle has made possible to extend this analysis to high order Fourier coefficients v_n with $n > 2$. As shown by theoretical calculations the sources for these momentum anisotropies v_n are fluctuations in the initial geometry [6–9]. The comparison between experimental data and event-by-event viscous hydrodynamic calculations have shown that the expected range of viscosity explored from RHIC to LHC energies is about $4\pi \langle \eta/s \rangle \sim 1 - 3$ [8, 9]. However there are several theoretical indications that η/s should have a particular temperature dependence [10, 11, 13–15]. As an example in Fig.1 shows a collection of theoretical results about the T dependence of η/s . Therefore a phenomenological estimation of the T dependence of η/s could give more information if the matter created in these collisions undergoes a phase transition [10, 11, 16]. More recently within viscous hydrodynamic calculation have been studied the correlations between the initial anisotropies, measured by the eccentricities ϵ_n , and the final anisotropies in momentum space v_n [17–19]. In general it has been shown that the degree of correlation between ϵ_n and v_n for a fixed centrality decrease with the order of the harmonic n .

In this proceeding we show the effects of the $\eta/s(T)$ on the $v_n(p_T)$ and we study the correlations between the initial ϵ_n and the final v_n by using a cascade approach with initial state fluctuations [20].

2 Kinetic approach at fixed $\eta/s(T)$

We have employed a relativistic transport code developed in these years to perform studies of the dynamics of heavy-ion collisions at both RHIC and LHC energies [3, 20, 25–28]. We solve numerically the RBT equation using the so called test particle method while for the collision integral we use the Monte Carlo methods, for details see [3, 25, 29].

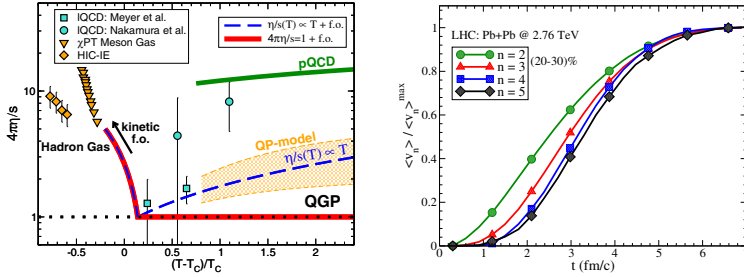


Figure 1: Left panel: $\eta/s(T)$ parametrizations. The light blue symbols are IQCD data [14, 21]. The orange symbols are for chiral perturbation theory [12, 13] and the phenomenological analysis for HIC at intermediate energy (HIC-IE) [22, 23]. The green line refers to pQCD calculations [24]. Right panel: $\langle v_n \rangle / \langle v_n \rangle^{\max}$ as a function of time for (20 – 30)%. Different symbols are for different harmonics n .

In the standard use of the transport theory one fixes the microscopical details of the scattering like cross sections of the processes to study the effect on the observables. In the following discussion we invert the description not in terms of fixed cross section σ_{tot} but in terms of fixed η/s . We simulate a system at fixed $\eta/s(T)$ by evaluating in each grid cell the total cross section σ_{tot} needed to have the wanted local viscosity. For a pQCD inspired cross section where $d\sigma/dt \sim \alpha_s^2/(t - m_D^2)^2$ with m_D being the screening mass regulating the angular dependence of the cross section, the η/s in the Chapman-Enskog theory is given by the following expression:

$$\eta/s = \frac{1}{15} \langle p \rangle \tau_\eta = \frac{1}{15} \frac{\langle p \rangle}{g(a) \sigma_{tot} \rho}, \quad (1)$$

with $a = m_D/2T$ while $g(a)$ is a function that take into account for the pertinent relaxation time $\tau_\eta^{-1} = g(a) \sigma_{tot} \rho$ associated to the shear transport coefficient. The function $g(a)$ it is given by: $g(a) = \frac{1}{50} \int dy y^6 \left[(y^2 + \frac{1}{3}) K_3(2y) - y K_2(2y) \right] h\left(\frac{a^2}{y^2}\right)$ where K_n -s are the Bessel functions. The function h relate the transport cross section to the total cross section $\sigma_{tr}(s) = \sigma_{tot} h(m_D^2/s)$ with $h(\zeta) = 4\zeta(1+\zeta)[(2\zeta+1)\ln(1+1/\zeta) - 2]$.

In Fig.1 it is shown the T dependence expected for η/s . The solid and dashed lines are the two parametrization considered in this work. As shown the η/s ratio is expected to increase at low temperature towards the estimated value for hadronic matter $4\pi\eta/s \approx 6$. Within this approach we have a self-consistent implementation of the kinetic freeze-out with a smooth switching-off of the scattering rates at low temperature, see [3, 20, 27].

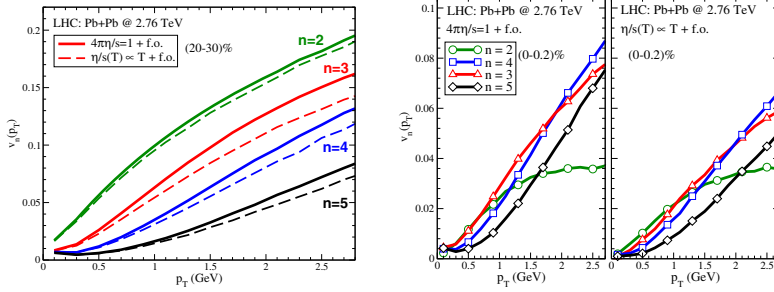


Figure 2: Left panel: $v_n(p_T)$ at mid rapidity for (20 – 30)%. Solid lines correspond to $\eta/s = (4\pi)^{-1}$ in QGP phase while dashed lines to $\eta/s \propto T$ in QGP phase. Right panel: comparison between $v_n(p_T)$ at mid rapidity for (0 – 0.2)% and for different T dependence of η/s . Different symbols are for different harmonics n .

3 Anisotropic flows $v_n(p_T)$ and correlations

We will show the results for $Au + Au$ collisions at $\sqrt{s_{NN}} = 200 \text{ GeV}$ produced at RHIC and $Pb + Pb$ collisions at $\sqrt{s_{NN}} = 2.76 \text{ TeV}$ at LHC. The implementation of initial state fluctuations in a transport cascade approach is made by using a Monte-Carlo Glauber model. Within this approach we determine initial distribution of the participant nucleons. The discrete distribution for the nucleons is converted in a smooth one by assuming for each nucleon a gaussian distribution. The width it has been fixed to $\sigma_{xy} = 0.5 \text{ fm}$. The density in the transverse plane $\rho_T(x, y)$ is given by the following sum $\rho_T(x, y) \propto \sum_{i=1}^{N_{part}} \exp[-\frac{(x-x_i)^2 + (y-y_i)^2}{2\sigma_{xy}^2}]$. In this way we generate an initial density profile that change event-by-event. For the initialization in momentum space at RHIC (LHC) energies we have considered a thermalized spectrum for partons with transverse momentum $p_T \leq p_0 = 2 \text{ GeV}$ (3 GeV). The initial local temperature in the transverse plane $T(x, y)$ is given by standard thermodynamical relation $\rho_T(x, y) = \gamma T^3 / \pi^2$ with $\gamma = 40$. The central region of the fireball for mid peripheral collision can reach temperature $T \approx 300 \text{ MeV}$ at RHIC and $T \approx 400 \text{ MeV}$ at LHC. While for partons with $p_T > p_0$ we assume the spectrum of non-quenched minijets according to standard NLO-pQCD calculations [30]. The initial time of the simulation is $\tau_0 = 0.6 \text{ fm}/c$ for RHIC and $\tau_0 = 0.3 \text{ fm}/c$ for LHC. For a detailed discussion about the implementation of the initial condition see [20]. In the right panel of Fig.1 it is shown the time evolution of the v_n normalized to their maximum. As shown different v_n have a different formation time. In particular harmonics with larger n develop later [20]. This imply that differ-

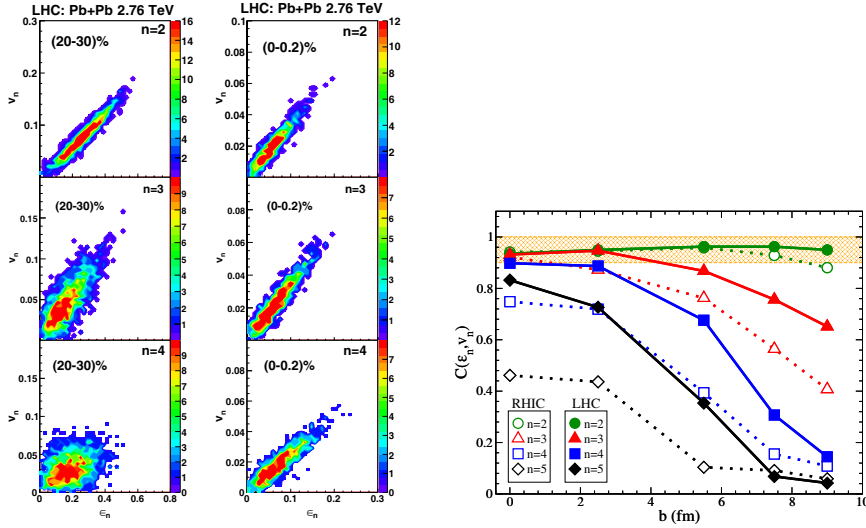


Figure 3: Left panel: Correlation plots between the initial eccentricities ϵ_n and final v_n at LHC energies and for two centralities (20 – 30)% and (0 – 0.2)%. In these calculations we have considered $\eta/s = 1/(4\pi)$ for high temperature and the kinetic f.o. at lower temperature (see red solid line in Fig.1). Right panel: $C(\epsilon_n, v_n)$ as a function of the impact parameter b . Different symbols refer to different harmonics n . The dotted (solid) lines are for RHC (LHC).

ent v_n develop in different stages of the fireball evolution and therefore they can probe different values of the η/s of the QGP. This means that each v_n have a different sensitivity to the T dependence of $\eta/s(T)$. As shown in the left panel of Fig.2 for mid-peripheral collisions the effect of the increase of η/s at high temperature is to reduce the $v_n(p_T)$ and the reduction is about of 10 %. In ultra-central collisions (see right panel of Fig.2) the sensitivity to $\eta/s(T)$ is strongly enhanced and we observe a reduction of $v_n(p_T)$ of about 30 – 35% for $n > 3$. This sensitivity increase with the order of the harmonics n . Moreover the p_T dependence of $v_n(p_T)$ change with the centrality. In fact as shown in Fig.2 for mid-peripheral collisions we observe that larger is n smaller is the corresponding anisotropic flow. In ultra-central collisions the ordering occurs only at low $p_T < 1 GeV$ where $v_n(p_T) \propto p_T^n$. At higher p_T the $v_n(p_T)$ are approximatively linear in p_T for $n \geq 3$ while we observe a saturation for $v_2(p_T)$ similar to that observed experimentally.

In the following discussion we show the results of correlations between the initial ϵ_n and the final v_n . The following results have been obtained with $N_{event} = 1000$ events for each centrality class with a total number of

test particle per event of $N_{test} = 2 \cdot 10^6$. In the correlation plots shown in left panel of Fig.3 we compare the degree of correlation between ϵ_n and v_n for $(0 - 0.2)\%$ and $(20 - 30)\%$. The results are for LHC energies. In the upper panel we observe a strong linear correlation between ϵ_2 and v_2 for both centralities. In agreement with viscous hydrodynamics [19]. In the middle and lower panel of Fig.3 it has been shown the correlation between ϵ_3 and v_3 and between ϵ_4 and v_4 respectively. For both cases we observe a reduction of the degree of correlation with the centrality. The correlation between ϵ_3 and v_3 for all the centralities is weaker with respect to that obtained for ϵ_2 and v_2 . Furthermore the v_4 shows a even a weaker degree of correlation with the initial ϵ_4 where for mid-peripheral collisions approximatively they are decorrelated. Similar behavior we observe at RHIC energies. To quantify the degree of correlation between ϵ_n and v_n we have studied the linear correlation coefficient $C(\epsilon_n, v_n)$ as a function of the impact parameter for both RHIC (dotted lines) and LHC energies (solid lines). Where $C(\epsilon_n, v_m)$ is given by:

$$C(\epsilon_n, v_m) = \frac{\sum_i (\epsilon_n^i - \langle \epsilon_n \rangle)(v_m^i - \langle v_m \rangle)}{\sqrt{\sum_i (\epsilon_n^i - \langle \epsilon_n \rangle)^2 \sum_i (v_m^i - \langle v_m \rangle)^2}} \quad (2)$$

the ϵ_n^i and v_m^i are the values of ϵ_n and v_m corresponding to the given event i . $C(\epsilon_n, v_n)$ is a decreasing function of the impact parameter for all the harmonics n , see Fig.3. We observe that for the second harmonic the correlation coefficient $C(\epsilon_2, v_2) \approx 1$ for all the range of impact parameter studied and for both RHIC and LHC. A lower correlation is observed for $n > 3$ where for example $C(\epsilon_5, v_5) < 0.5$ for all centralities. The comparison between dotted and solid lines show that at LHC there is more correlation than at RHIC. In particular at LHC and for ultra-central collisions $C(\epsilon_n, v_n) > 0.9$ for $n = 2, 3, 4$ as shown by the orange band. This behavior suggest that the value obtained for $\langle v_n \rangle$ are strongly related to the initial value of ϵ_n .

4 Conclusions

We have studied the effect of the η/s on the anisotropic flows $v_n(p_T)$ for $n = 2, 3, 4$ and 5 within an event-by-event transport approach. We found that at LHC energies and for mid-peripheral collisions there is a weak sensitivity of $v_n(p_T)$ to the T dependence in the QGP phase. An interesting result we observe for ultra-central collisions where found an enhancement of the sensitivity of the $v_n(p_T)$. This sensitivity increase with the order of the harmonics n and for $n = 5$ it reaches about a 30%.

Finally, the study of the correlations between the initial eccentricities ϵ_n , and the final anisotropic flows $\langle v_n \rangle$ shows that $C(\epsilon_n, v_n)$ is a decreasing function of the impact parameter. Moreover larger is the collision energy larger is the degree of correlation and at LHC there is significantly more correlation than at RHIC. In particular at LHC energies and for ultra-central collisions (0 – 0.2%) we found that $C(\epsilon_n, v_n) > 0.9$ up to the 4-th harmonic. This strong linear correlation imply that the $v_n \propto \epsilon_n$ and it suggests that the study of v_n can give information about the initial geometry of the fireball.

Acknowledgments

V.Greco, S. Plumari, F. Scardina and G.L. Guardo acknowledge the support of the ERC-StG Grant under the QGPDyn project.

References

- [1] Romatschke P and Romatschke U 2007 *Phys.Rev.Lett.* **99** 172301.
- [2] Song H and Heinz U W 2008 *Phys.Rev.* **C78** 024902.
- [3] Ferini G, Colonna M, Di Toro M and Greco V 2009 *Phys.Lett.* **B670** 325.
- [4] Xu Z and Greiner C 2009 *Phys.Rev.* **C79** 014904.
- [5] Kovtun P, Son D and Starinets A 2005 *Phys.Rev.Lett.* **94** 111601.
- [6] Qin G Y, Petersen H, Bass S A and Muller B 2010 *Phys.Rev.* **C82** 064903.
- [7] Holopainen H, Niemi H and Eskola K J 2011 *Phys.Rev.* **C83** 034901.
- [8] Schenke B, Jeon S and Gale C 2012 *Phys.Rev.* **C85** 024901.
- [9] Gale C, Jeon S, Schenke B, Tribedy P and Venugopalan R 2013 *Phys.Rev.Lett.* **110** 012302.
- [10] Csernai L P, Kapusta J and McLerran L D 2006 *Phys.Rev.Lett.* **97** 152303.
- [11] Lacey R A, Ajitanand N, Alexander J, Chung P, Holzmann W *et al.* 2007 *Phys.Rev.Lett.* **98** 092301.

-
- [12] Prakash M, Prakash M, Venugopalan R and Welke G 1993 *Phys.Rept.* **227** 321.
- [13] Chen J W, Li Y H, Liu Y F and Nakano E 2007 *Phys.Rev.* **D76** 114011.
- [14] Meyer H B 2007 *Phys.Rev.* **D76** 101701.
- [15] Das S K and Alam J e 2011 *Phys.Rev.* **D83** 114011.
- [16] Plumari S, Greco V and Csernai L 2013 arXiv:1304.6566.
- [17] Gardim F G, Grassi F, Luzum M and Ollitrault J Y 2012 *Phys.Rev.* **C85** 024908.
- [18] Chaudhuri A, Haque M R, Roy V and Mohanty B 2013 *Phys.Rev.* **C87** 034907.
- [19] Niemi H, Denicol G, Holopainen H and Huovinen P 2013 *Phys.Rev.* **C87** 054901.
- [20] Plumari S, Guardo G L, Scardina F and Greco V 2015 arXiv:1507.05540.
- [21] Nakamura A and Sakai S 2005 *Phys.Rev.Lett.* **94** 072305.
- [22] Schmidt W, Katscher U, Waldhauser B, Maruhn J, Stocker H *et al.* 1993 *Phys.Rev.* **C47** 2782.
- [23] Danielewicz P, Barker B and Shi L 2009 *AIP Conf.Proc.* **1128** 104.
- [24] Arnold P B, Moore G D and Yaffe L G 2003 *JHEP* **0305** 051.
- [25] Plumari S, Puglisi A, Scardina F and Greco V 2012 *Phys.Rev.* **C86** 054902.
- [26] Ruggieri M, Scardina F, Plumari S and Greco V 2013 *Phys.Lett.* **B727** 177.
- [27] Ruggieri M, Scardina F, Plumari S and Greco V 2014 *Phys.Rev.* **C89** 054914.
- [28] Plumari S, Guardo G L, Greco V and Ollitrault J Y 2015 *Nucl. Phys.* **A941** 87.
- [29] Xu Z and Greiner C 2005 *Phys.Rev.* **C71** 064901.
- [30] Greco V, Ko C and Levai P 2003 *Phys.Rev.* **C68** 034904.